

**DOSIMETRIC AND GEOMETRIC ACCURACY  
OF IMAGE GUIDED INTENSITY MODULATED  
RADIOTHERAPY (IG-IMRT) IN HEAD AND  
NECK CANCER PATIENTS**

**NADA ‘ALIA BINTI M ZAMRI**

**UNIVERSITI SAINS MALAYSIA**

**2019**

**DOSIMETRIC AND GEOMETRIC ACCURACY  
OF IMAGE GUIDED INTENSITY MODULATED  
RADIOTHERAPY (IG-IMRT) IN HEAD AND  
NECK CANCER PATIENTS**

by

**NADA ‘ALIA BINTI M ZAMRI**

**Thesis submitted in fulfilment of the requirement  
for the degree of  
Master of Science**

**July 2019**

## **ACKNOWLEDGEMENT**

I would like to sincerely thank my supervisor, Dr Mohd Hafiz B Mohd Zin and my co-supervisor, Dr Shazril Imran B Shaukat for their guidance and mentoring throughout the project. I am indebted to their wealth of experience and am grateful to their encouragement. I also want to express my gratitude to the radiotherapists, medical physicists and oncologist of Oncology and Radiotherapy Department, Advanced Medical and Dental Institute for their cooperation in completing the project. Special thanks also to my family and friends for their support in completing this project.

## TABLES OF CONTENTS

<b>ACKNOWLEDGEMENT</b>	ii
<b>TABLES OF CONTENTS</b>	iii
<b>LIST OF TABLES</b>	vi
<b>LIST OF FIGURES</b>	vii
<b>LIST OF ABBREVIATIONS</b>	xi
<b>ABSTRAK</b>	xiii
<b>ABSTRACT</b>	xiv
<b>CHAPTER 1 - INTRODUCTION</b>	<b>1</b>
1.1 Introduction to radiotherapy	1
1.1.1 Radiotherapy linear accelerator	2
1.1.2 Radiotherapy treatment flow	5
1.2 Intensity Modulated Radiotherapy (IMRT)	9
1.2.1 Patient specific IMRT QA	10
1.2.2 Dosimetric accuracy for IMRT verifications	11
1.2.3 Method for patient specific IMRT QA for treatment verification	12
1.3 Geometrical uncertainties in radiotherapy	13
1.3.1 Margin recipe	14
1.3.2 Image guided radiotherapy (IGRT)	15
1.3.2(a) Cone-beam computed tomography (CBCT)	16
1.3.2(b) Correction strategies with image guided radiotherapy	17
1.4 Dosimetric impact of geometrical uncertainties on dose distributions	19
1.5 Purpose of study	20
<b>CHAPTER 2 - MATERIALS AND METHODS</b>	<b>21</b>
2.1 Radiotherapy and dosimetry system	21
2.1.1 Radiotherapy linac and quality assurance	21
2.1.2 Treatment planning system (TPS)	23
2.1.3 Radiation detector for IMRT verification	23
2.1.4 Characterisation of the ionisation chamber array detector	24
2.2 Patient specific IMRT QA	29
2.2.1 Patient characteristics	29
2.2.2 Radiotherapy simulation and planning	30

2.2.3	Patient specific QA for IMRT treatment plan verification	32
2.3	Setup accuracy of patients using CBCT based-IGRT	34
2.3.1	Setup and image registration	34
2.3.2	Analysis of setup errors	35
2.3.2(a)	Description of setup error	35
2.3.2(b)	Systematic and random errors	36
2.3.2(c)	Determination of PTV margin	37
2.3.3	IGRT correction strategies/protocols	37
2.3.3(a)	Online protocol	37
2.3.3(b)	Offline protocol	38
2.4	Impact of setup errors on the dose distribution	40
2.4.1	Remodelling of PTV dose	40
2.4.2	Simulation of impact of setup errors on dose distribution	41
2.4.3	Gamma analysis	43
2.4.4	Dose-Volume Histogram (DVH) analysis	43
<b>CHAPTER 3 - RESULTS AND DISCUSSION</b>		<b>46</b>
3.1	Radiotherapy and dosimetry system	46
3.1.1	Quality assurance (QA) of linac	46
3.1.2	Characterisation of the dosimetry system	47
3.1.2(a)	Output factor	47
3.1.2(b)	Linearity	49
3.1.2(c)	Dose rate dependency	50
3.1.2(d)	Directional dependency	50
3.1.2(e)	Source-to-surface distance (SSD) dependency	51
3.1.2(f)	Reproducibility	52
3.1.2(g)	Summary of characterisation study	53
3.2	Patient specific IMRT QA	54
3.3	Setup uncertainty using CBCT-based IGRT	56
3.3.1	Analysis of setup error without IGRT correction	56
3.3.2	Analysis of setup error after the application of IGRT correction	59
3.3.2(a)	Online IGRT correction	59
3.3.2(b)	Offline IGRT protocol	60
3.3.3	Comparison between setup error and with/without IGRT protocol	61
3.3.3(a)	Systematic error	61

3.3.3(b) Random error	66
3.3.3(c) Setup error versus timeline	70
3.3.3(d) Determination of PTV margin	71
3.4 Impact of setup errors towards dose distribution of head and neck cancer patients	73
3.4.1 Gamma analysis	73
3.4.2 Dose-Volume Histogram (DVH) analysis	78
<b>CHAPTER 4 - SUMMARY AND CONCLUSION</b>	<b>91</b>
4.1 Conclusions	91
4.2 Recommendations and future work	93
<b>REFERENCES</b>	<b>95</b>
<b>APPENDIX</b>	

## LIST OF TABLES

		<b>Page</b>
Table 1.1	Summary of published safety margin recipes for target	19
Table 2.1	Patient and treatment characteristics	30
Table 2.2	Example of measuring setup error from several patients	35
Table 2.3	Dose of equivalent PTVs for all six HNC patients	41
Table 2.4	98% of dose threshold of each PTVs levels	45
Table 3.1	QA results for linac parameters	46

## LIST OF FIGURES

		Page
Figure 1.1	Linear accelerator from Elekta	4
Figure 1.2	Schematic diagram of gantry head of linac	4
Figure 1.3	Schematic diagram of target delineation recommended	8
Figure 1.4	Example of radiographic image of head and neck cancer from Monaco TPS in AMDI, USM	9
Figure 1.5	Example of multileaf collimator	10
Figure 1.6	Example of ion chamber detector array system. A PTW 2D Array Seven29 ion chamber	13
Figure 2.1	X-ray volume imaging (XVI) software	22
Figure 2.2	CT scan images of the phantom and detector from TPS	27
Figure 2.3	Experimental setup of ionisation chamber array detector	28
Figure 2.4	Octavius phantom is ensured to aligned perpendicularly with the in-room laser	29
Figure 2.5	The immobilisation system for HNC patients	33
Figure 2.6	The comparison of measured and calculated dose map using Verisoft software	34
Figure 2.7	Flowchart of online IGRT protocol	38
Figure 2.8	Flowchart of offline IGRT protocol	39
Figure 2.9	Simulation of dose maps based on setup error and after Offline IGRT protocol	42
Figure 2.10	Process of obtaining 98% of dose threshold for each CTVs	44



Figure 3.1	Output factor comparison between ionisation chamber array detector and TPS	48
Figure 3.2	Linearity test for ionisation chamber array detector and TPS. The results of linear regressions for both TPS and detector (dashed line) are also shown	49
Figure 3.3	Dose rate of ionisation chamber array from 100 MU/min to 600 MU/min	50
Figure 3.4	The comparison of output dose at different angle from 0° to 360° between ionisation chamber array detector and TPS	51
Figure 3.5	Dose output comparison between ionisation chamber array detector and TPS from SSD 80 cm to 120 cm.	52
Figure 3.6	Pass rate report at different gamma criteria for each measurements of ionisation chamber array detector taken	53
Figure 3.7	IMRT pre-treatment verification result obtained when comparing the dose measured from ionisation chamber array detector with the dose calculated from TPS at different gamma criteria.	55
Figure 3.8	The range of setup errors of 231 CBCT images in RL, SI and AP direction	57
Figure 3.9	Scattered plot illustrating individual mean setup errors in (i) RL, (ii) SI and (iii) AP directions. The dashed line denoted population mean was plotted for each diagram.	58
Figure 3.10	The individual mean errors of all patients in RL direction	63
Figure 3.11	The individual mean errors of all patients in SI direction	64
Figure 3.12	The individual mean errors of all patients in AP direction	65

Figure 3.13	The individual random errors observed in RL direction	67
Figure 3.14	The individual random errors observed in SI direction	68
Figure 3.15	The individual random errors observed in AP direction	69
Figure 3.16	Random error before and after application of IGRT correction	70
Figure 3.17	Example of setup error versus fraction in SI direction	71
Figure 3.18	Comparison of gamma pass rate report between dose maps with setup error, dose map shifted based on NAL correction and dose map shifted based on eNAL correction at 3%/3 mm gamma criteria	75
Figure 3.19	Comparison of gamma pass rate report between dose maps with setup error, dose map shifted based on NAL correction and dose map shifted based on eNAL correction at 2%/2 mm gamma criteria	76
Figure 3.20	Comparison of gamma pass rate report between dose maps with setup error, dose map shifted based on NAL correction and dose map shifted based on eNAL correction at 1%/1 mm gamma criteria	77
Figure 3.21	Dose map that represent 95% dose threshold of CTV1 for patient 1	79
Figure 3.22	Dose map that represent 95% dose threshold of CTV2 for patient 1	80
Figure 3.23	Dose map that represent 95% dose threshold of CTV3 for patient 1	81

Figure 3.38	Dose volume histogram for CTV1, CTV2 and CTV3 for patient 1	83
Figure 3.39	Dose volume histogram for CTV1, CTV2 and CTV3 for patient 2	84
Figure 3.40	Dose volume histogram for CTV1, CTV2 and CTV3 for patient 3	85
Figure 3.41	Dose volume histogram for CTV1, CTV2 and CTV3 for patient 4	86
Figure 3.42	Dose volume histogram for CTV1, CTV2 and CTV3 for patient 5	87
Figure 3.43	Dose volume histogram for CTV1, CTV2 and CTV3 for patient 6	88
Figure 3.44	The error difference at 98% of dose threshold for each CTVs level; a) CTV3, b) CTV2 and c) CTV1.	90

## LIST OF ABBREVIATIONS

2D	two-dimensional
3D	three-dimensional
AAPM	American Association of Physicist in Medicine
AP	anterior-posterior
ASTRO	American Society of Radiation Oncology
CBCT	Cone beam computed tomography
CT	Computed tomography
CTV	clinical target volume
CRT	conformal radiotherapy
DD	dose difference
DTA	distance to agreement
DVH	dose-volume histogram
EBRT	external beam radiotherapy
eNAL	extended no action level
EPID	electronic portal imaging device
FPI	flat panel imager
GTV	gross tumour volume
HNC	head and neck cancer
ICRU	International Commission on Radiation Unit and Measurements
IGRT	Image Guided Radiotherapy
IMRT	Intensity Modulated Radiotherapy
kV	kilovoltage
LINAC	linear accelerator
MRI	Magnetic resonance imaging
MLC	multileaf collimator

MU	monitor unit
MV	megavoltage
NAL	no action level
OAR	organ at risk
OBI	on-board imager
PET	Positron emission tomography
PTV	planning target volume
QA	quality assurance
RMS	root mean square
RL	right-left
SD	standard deviation
SI	superior-inferior
SSD	source to surface distance
TG	Task Group
TPS	treatment planning system
WHO	World Health Organisation
XVI	X-ray Volume Imager

**KETEPATAN DOSIMETRI AND GEOMETRI UNTUK RADIOTERAPI  
MODULASI KEMATAN-BERPANDUKAN IMEJ (IG-IMRT) BAGI  
PESAKIT TUMOR KEPALA DAN LEHER**

**ABSTRAK**

Kemajuan dalam teknologi radioterapi telah membolehkan radioterapi modulasi kamatan (IMRT) untuk merawat pesakit dengan ketepatan kedudukan pesakit yang lebih baik menggunakan radioterapi berpandukan imej (IGRT). Kajian ini menyiasat ketepatan IG-IMRT merawat 25 pesakit kanser kepala dan leher (HNC) di Institut Perubatan dan Pergigian Termaju (IPPT), Universiti Sains Malaysia. Sebuah detektor susun-atur kebuk ion telah diperkenalkan dan digunakan untuk verifikasi pelan rawatan IMRT. Kajian percirisan menunjukkan dos yang diukur menggunakan detektor susun-atur kebuk ion mempunyai perbezaan  $<2\%$  dengan dos yang dikira dari sistem perancangan rawatan (TPS). Semua 25 pelan pesakit IMRT mencatatkan kadar peratusan lulus  $\geq 95\%$  apabila kriteria gama  $3\%/3\text{ mm}$  digunakan. Sebanyak 231 CBCT imej telah diperolehi selepas persediaan pesakit sebelum rawatan IMRT dimulakan. Margin PTV  $\geq 3\text{ mm}$  diperlukan dalam arah RL, SI dan AP jika tiada pembetulan persediaan dilakukan. Protokol NAL dan eNAL disimulasikan dalam ralat persediaan. Protokol eNAL merekodkan ralat persediaan yang terkecil dalam kesemua tiga arah yang dikaji iaitu  $1.59\text{ mm}$  untuk RL,  $2.13\text{ mm}$  untuk SI dan  $1.61\text{ mm}$  untuk AP. Kesan ralat persediaan pada dos pengagihan juga dinilai pada 6 pesakit HNC terpilih. Penggunaan protokol eNAL berupaya meningkatkan peratus kawasan menerima sekurang-kurang  $95\%$  daripada dos yang ditetapkan sebanyak  $0.12\%$ ,  $0.15\%$  dan  $0.80\%$  untuk CTV1, CTV2 dan CTV3 berbanding peta dos tanpa pembetulan ralat kedudukan pesakit.

# **DOSIMETRIC AND GEOMETRIC ACCURACY OF IMAGE GUIDED INTENSITY MODULATED RADIOTHERAPY (IG-IMRT) IN HEAD AND NECK CANCER PATIENTS**

## **ABSTRACT**

Advances in radiotherapy technology has made it possible to deliver highly conformal Intensity Modulated Radiotherapy (IMRT) beam to treat patient with improved setup accuracy using Image Guided Radiotherapy (IGRT). This retrospective study investigates the accuracy of IG-IMRT treatment for 25 head and neck cancer (HNC) patients in Advanced Medical & Dental Institute (AMDI), Universiti Sains Malaysia. An ionisation chamber array detector has been characterised and used for patient specific IMRT QA. The characterisation study shows the doses measured using ionisation chamber array detector were within 2% compared with the doses calculated from the treatment planning system (TPS). All 25 IMRT treatment obtained percentage pass rate  $\geq 95\%$  when 3%/3 mm gamma criteria were used. The geometrical accuracy of the treatment was also analysed based on setup errors measured using kV cone beam CT based-IGRT. A total of 231 pre-treatment CBCT imaging were acquired prior to treatment and compared to the reference CT. PTV margin of  $\geq 3$  mm in RL direction, SI direction and AP direction is required if no setup correction was performed. Offline setup protocols; NAL and eNAL were simulated on the setup errors recorded. The eNAL protocol recorded the smallest setup error in all three directions; which were 1.59 mm for RL direction, 2.13 mm for SI direction and 1.61 mm for AP direction. The impact of setup errors on dose distributions was also assessed on six HNC patients. The eNAL protocol improved

target coverage with 0.12%, 0.15% and 0.80% higher volume of CTV1, CTV2 and CTV3 region, respectively receiving at least 95% of prescribed dose compared to without setup error correction. Therefore, setup error correction is important to ensure the precise delivery of radiotherapy treatment by reducing both systematic and random errors which resulted a better coverage of tumour volume to be irradiated. In conclusion, CBCT-based IGRT correction technique is an effective method to further improve the accuracy of IMRT treatment in HNC patient.



# **CHAPTER 1 INTRODUCTION**

## **1.1 Introduction to radiotherapy**

Cancer has become one of the most common diseases in the world according to World Health Organisation (WHO). Death worldwide caused by cancer is 8.8 million in 2015 [1]. According to the latest National Cancer Registry of Malaysia (NCR), a total number of 103,507 new cancer cases were diagnosed in Malaysia during the period of 2007 to 2011 [2]. The incidence of new cases is increasing which may be attributed to increase in general life expectancy, change in dietary intake and lifestyle, improvements in diagnostics technology for early detection and also increased access to healthcare system from rural areas [3,4].

With ever increasing number and complexity of cancer cases, radiotherapy has become one of the important treatment modalities in treating cancer. Radiotherapy treatment is delivered either as a standalone treatment or in combination with chemotherapy and/or surgery. The main objective of radiotherapy treatment is to accurately deliver radiation dose to the tumour target in order to destroy cancer cells and at the same time minimising the radiation dose to normal tissues surrounding the tumour. Radiation may be delivered from radioactive source internally dwelled into the body which is known as brachytherapy or externally using machine to delivered radiation to penetrate the body known as external beam radiotherapy (EBRT). EBRT is the focus of the work and will be referred to as radiotherapy throughout the thesis. Radiotherapy can either be intended for curative to cure the patient from cancer, or as

an adjunct to other modalities to increase rates of cure and remission from cancer or as a palliative modality to symptomatically relief symptoms such as pain or bleeding.

### **1.1.1 Radiotherapy linear accelerator**

Radiotherapy uses a linear accelerator (linac) to generate high energy x-rays and electrons to conform to the planned target while sparing surrounding normal tissues. A linac consists of a rotating gantry head and treatment couch as shown in Figure 1.1. Modern linac also has a kV x-ray unit located at the left arm of the linac and a detector, located at the right arm of the linac. The kV x-ray unit is also known as cone-beam computed tomography (CBCT). It provides a high-quality verification image at the treatment site. The technique is called image guided radiation therapy (IGRT). This will further be discussed in section 1.3.

High energy x-ray photons are generated from the gantry head of linac is showed in Figure 1.2. Electrons are generated from the heating of filament within the electron gun (cathode). The electrons are then injected to the tube structure called the accelerator waveguide and accelerates along it with almost the speed of light. The electron beam then enters a flight tube which contains bending magnet. The bending magnet will direct the electron beam towards the target. The electron beams accelerated and its kinetic energy increased until it collides with the target. The interaction produces Bremsstrahlung x-ray photons.

Some of the high energy photons which emerge from the target pass through a primary collimator of the linac. A beam flattening flatter is placed in the path of photons to absorb more forward peaking photons than the ones in periphery. The filter helps in shaping the photon beams in its cross-sectional dimensions to a more uniform beam.

Two ionisation chambers are located below the flattening filter to monitor integrated dose, dose rate and also field symmetry. The radiation beams that leave the x-ray target or the flattening filter will pass through the dual monitor ionisation chambers and produce the ionisation current. Once the photon beam passed the dual monitor ionisation chamber, the beam is shaped using a secondary collimator. The secondary collimator helps to deliver a beam that is more conformal to the tumour. The conventional beam shaping uses the combination of upper jaw and lower jaw and also beam blocks which attached to the accelerator to produce a rectangular or square field. However, this conventional method restricts the conformity of the beam as it only allows limited number of beam shape. The multileaf collimators (MLC) is used for a more flexible beam shaping system. They are heavy metal field-shaping device with independent moving mechanism that direct the radiation dose to the tumour. The MLCs are the key element in the treatment delivery of x-ray beams with intensity modulated radiotherapy (IMRT) which will be discuss further in section 1.2.

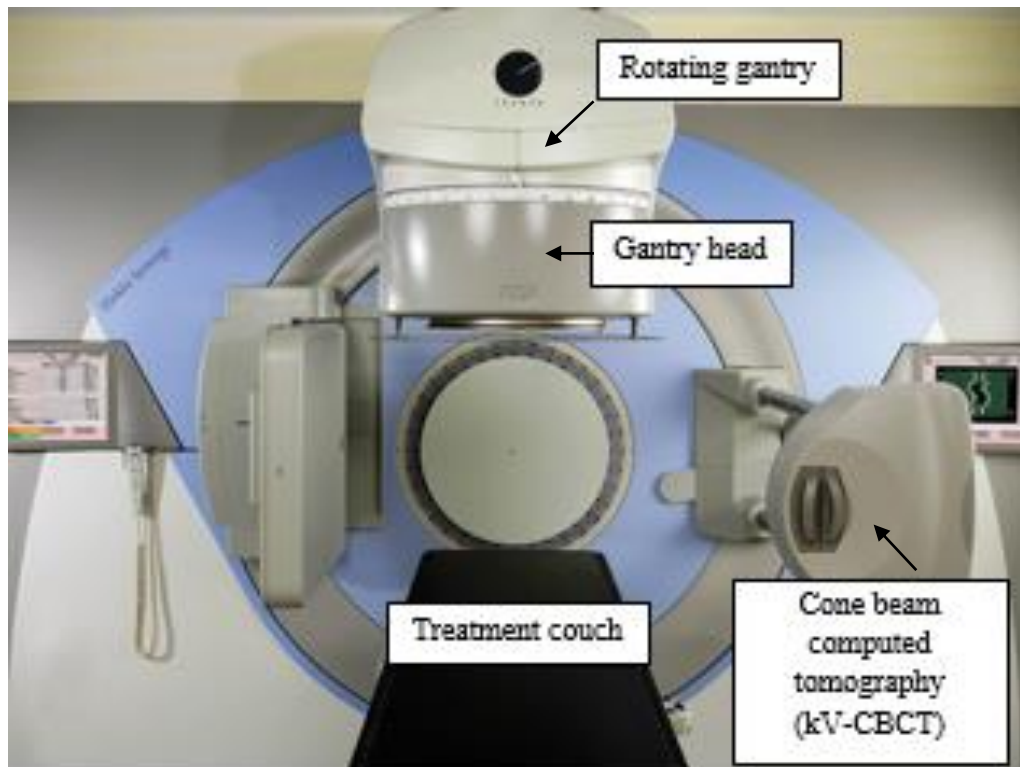


Figure 1.1: Linear accelerator from Elekta (Picture courtesy from [www.oncologysystems.com](http://www.oncologysystems.com))

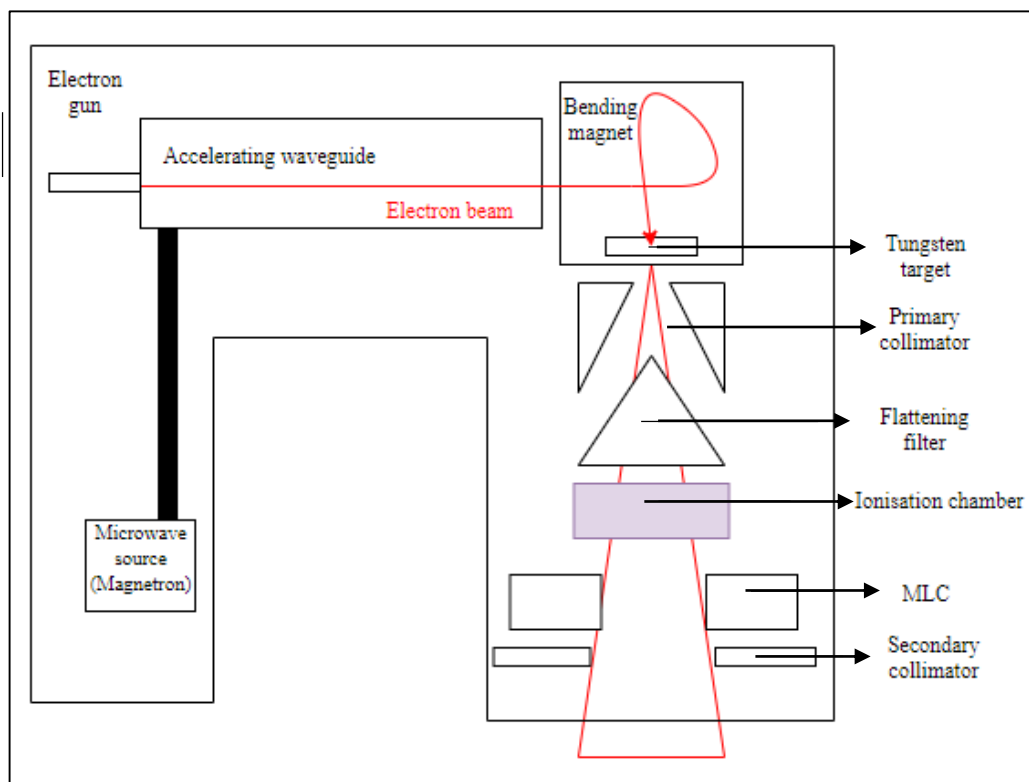


Figure 1.2: Schematic diagram of gantry head of lina

### **1.1.2 Radiotherapy treatment flow**

Modern conformal radiotherapy has evolved from using bony anatomy as surface landmarks for hand-drawn blocking towards specialised planning that incorporates three-dimensional (3D) reconstructed images with computer optimisation algorithms for dose calculation. The conventional radiotherapy treatment of two-dimensional (2D) radiotherapy contains a single beam. The beam setups for conventional radiotherapy are quite simple because the plans are either consisted of opposed lateral fields or four field “boxes” [5]. Three-dimensional conformal radiotherapy (3D-CRT) and IMRT are more conformal radiotherapy treatment compared to 2D radiotherapy as they use collimators on linac to deliver accurate radiation doses to the target volume. However, compared to IMRT, 3D-CRT treatment planning system is manually optimised [6]. This means that the treatment planners have to decide all the beam parameters, such as the number of beams, beam directions, shapes, wedges and weightages for to obtain the desired dose distribution. After all the parameters have been set, only then the computer calculates the resulting dose distribution. Conversely, for IMRT treatment, the physicist only has to decide the desired dose distributions and some of the treatment parameters. The rest of the treatment parameters are calculated by the computerised treatment planning system.

There are several stages of process in radiotherapy treatment. When a patient is planned for radiotherapy, a computerised planning needs to be done to ensure precise dose is delivered to the target volume and sparing the critical structures near target volume. The patient is positioned in a comfortable reproducible position and this may require using immobilisation device such as thermoplastic mask to maintain position. Then, the images of the tumour position are acquired using computed tomography (CT) scanner for target delineation. Advanced imaging modalities such as Magnetic

Resonance Imaging (MRI), Positron Emission Tomography (PET) or PET/CT are used for more precise target delineation and better sparing of organ at risk (OAR). All images are then sent to a treatment planning system (TPS). Image fusion of different imaging modalities can also be done to ensure a more accurate and precise target delineation for the purpose of planning radiotherapy treatment.

Treatment planners consisted of oncologist and physicist will work together to contour the tumour region that need to be treated as well as OAR surrounding the tumour to be spared on the TPS. The oncologist delineates the structures of the target volumes and OARs on the images obtained from a CT scan or fused and registered with other imaging modalities. Thus, the main volumes to be considered while contouring are the gross tumour volume (GTV); a contour on gross radiologically visible tumour, the clinical target volume (CTV); tissues surrounding GTV that pathologically at high risk to contain subclinical malignant diseases and planning target volume (PTV); a geometric extension of CTV to account for setup errors during treatment and in between treatment motion. These tumour volumes are shown in Figure 1.3. The OARs are normal tissues surrounding the target volume that may receive unwanted radiation doses during treatment. These tumour delineation follows the recommendation by the International Commission on Radiation Unit and Measurements 62 (ICRU 62) [7].

After delineation process, the physicist needs to specify number of gantry angles and dose goals for target dose and OARs objectives in the inverse planning system. Normally, a physicist or a dosimetrist will set a constraint to the critical structures surrounding the target in order to instruct the TPS to consider keeping the dose of those regions low when planning the beams. This helps to guide optimisation process of IMRT planning which will take place once all doses have been prescribed

to contoured structures. The TPS dose calculation algorithms that can be used are Monte Carlo algorithm and pencil beam algorithm. The dose calculated will then be evaluated to ensure the treatment prescription is either achieved or not and the OAR dose limits are satisfied. A dose-volume histogram (DVH) will then be generated from TPS as a plan evaluation tool by the planner to evaluate doses to different structures. DVH is a histogram of radiation dose to tissue volume in radiotherapy treatment planning. It summarises the 3D dose distribution in a graphical 2D format. The "volumes" referred to in DVH analysis are the tumour target, OARs surrounding the target, or an arbitrary structure. This is to ensure that the planned treatment beam and dose prescription are able to cover the target volume and at the same time the organ at risks surrounding the target are spared.

Finally, once the dose distributions and DVHs have been reviewed by physicist and approved by oncologist, the treatment plan needs to be verified by modelling the treatment planned into a dosimeter and carry out the patient specific IMRT quality assurance (QA) which will be discussed further in section 1.2.1.

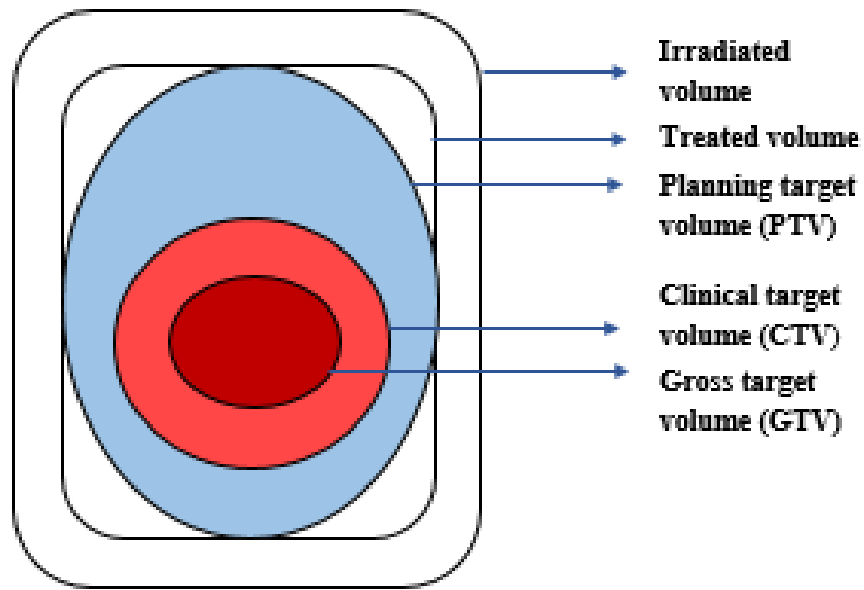


Figure 1.3: Schematic diagram of target delineation recommended by ICRU 62

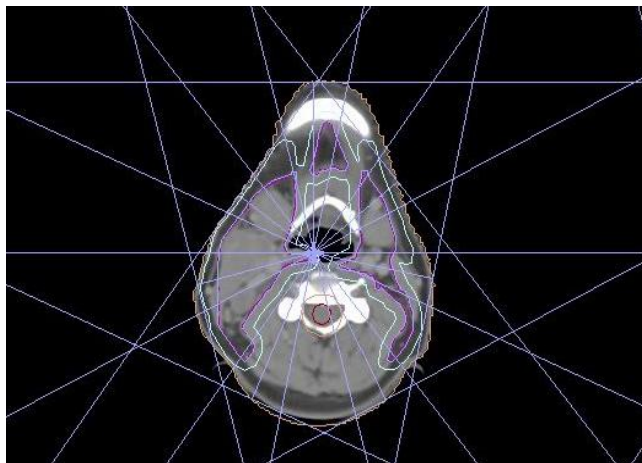


Figure 1.4: Example of CT image of head and neck cancer captured from Monaco TPS in AMDI, USM

The dosimetric accuracy is one of the radiotherapy challenges. The dosimetric inaccuracy may affect the treatment verification. There are several causes of



dosimetric inaccuracy such as linac delivery, dose calculation error and dosimeter error [8,9]. However, the factor of dosimetric inaccuracy that will be focussed in this study is the dosimeter error. If the dosimeter used for treatment verification lack of good characteristics such as linearity and directional dependence, the precision and accuracy of treatment verification may also be affected. The discussion on dosimetric accuracy will further be discussed under section 1.2.1 and 1.2.2.

Geometrical accuracy is also one of the challenges in radiotherapy. The geometrical accuracy may affect the patient setup which will then result in higher dose to organ at risks and lower dose to tumour target. Deviations in patient setup and organ motion are often become the limiting aspects to achieve the precision and accuracy of radiation delivery in IMRT [10]. The errors might arise due to immobilisation and setup uncertainty during patient positioning. Further discussion on the effect of geometrical accuracy will be discussed in section 1.3.

## **1.2 Intensity Modulated Radiotherapy (IMRT)**

IMRT is one of the advanced forms of radiotherapy treatments. IMRT uses collimators which is known as multi-leaf collimator (MLC) as shown in Figure 1.5 to deliver a conformal radiation dose. MLC has replaced the beam blocks in conventional method of field shaping. MLC consists of movable leaves arranged in two opposing rows. Step-and-shoot MLC can move in immobile position during beam off whereby dynamic MLC move continuously while the beam is on [11]. The movement of the MLC leaves help to generate a more complex beam shape to modify the beam intensity for IMRT treatment. The enhancement of the beam shaping technique ensures an efficient delivery of complex beam during IMRT treatment.

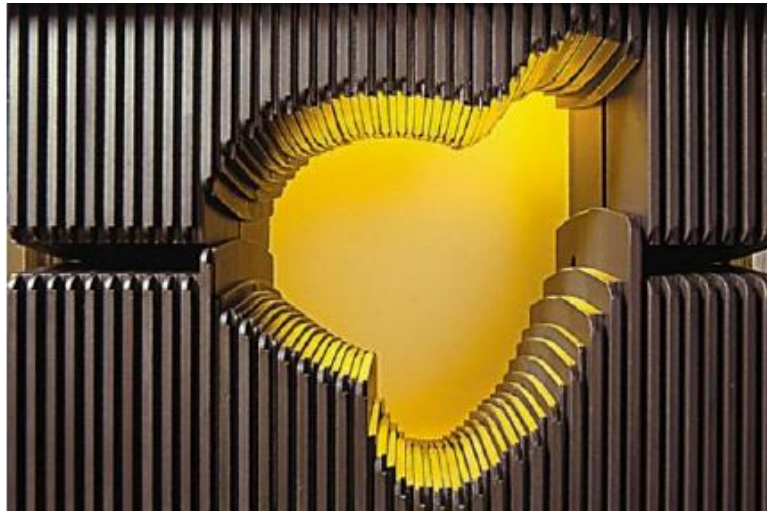


Figure 1.5 Example of multileaf collimator (Figure courtesy from Varian Medical System, [www.varianmediaroom.com](http://www.varianmediaroom.com))

Several recent studies have demonstrated how IMRT can improve dose to target tissues while sparing the surrounding normal tissues [12,13]. A study on IMRT dose sparing shows that xerostomia can be successfully prevented or reduced by restricting the maximum mean dose threshold to 26 Gy for at least one parotid gland [14]. Even though IMRT improves dose distributions to the target organs and decrease irradiation doses to normal tissue, the high conformality may also result in geographical misses and locoregional failures. Therefore, there is a need of proper delineation of tumour and sparing OARs [13].

### **1.2.1 Patient specific IMRT QA**

IMRT requires their dosimetric verification due to the complexity of the treatment plans. Therefore, before any IMRT treatment takes place, actual dose being delivered to the patient needs to be verified first [15]. The dose verification can be done using a phantom with calibrated system or films. There are various products that are commercially available today for IMRT verification such as flat-panel electronic portal

imaging devices (EPID) and ionisation chamber in the form of matrix or linear detector arrays. A pre-treatment patient specific dose verification is done to check on the accuracy of dose calculation and delivery system.

### **1.2.2 Dosimetric accuracy for IMRT verifications**

There is a need to validate individual IMRT treatment plans before the treatment is delivered on patients. This is due to the complexity of IMRT treatment that demands a stringent QA and accurate dose determination for delivery of highly conformal dose to the patients. Patient specific IMRT QA is performed by comparing the dose delivered to a dosimeter with the dose calculated by the TPS using the same treatment parameters [16]. The conventional method of performing pre-treatment patient specific dose verification is by using film [17,18]. For example, gafchromic film was normally used since it was the most cost-effective method and provided a good spatial resolution [19]. However, there were several problems when the film was being used for IMRT verification purpose as film requires 2D film density scanner to quantitatively convert optical density to dose [20]. Furthermore, film measurement involves difficult calibration [21]. Errors may be presented if the calibration process is not performed correctly. This calibration factor is important to ensure accurate conversion of the pixel values to the dose value.

Apart from film, the electron portal imaging device (EPID) has good spatial resolution and can provide real-time measurements. However, the sensitivity of EPID to MLC position error is low due to the imaging speed of EPID that is slow [22]. EPID response also changes with the cumulative exposure to radiation and requires frequent calibration [23]. The calibration algorithm requires noise correction to accurately convert the signal from EPID to dose [24].

In recent years, most clinics have been using a dosimetric phantom which is a detector array system in conjunction with solid water phantom. The ionisation chamber array detector allows real-time measurements and have become the gold standard tool for patient specific QA in advanced radiotherapy. The ionisation chamber array detector provides immediate results after beam delivery. Although the resolution of ionisation chamber detector array is limited, it provides undeviating measurement of dose without frequent calibration. An example of the ionisation chamber array detector system is shown in Figure 1.6.

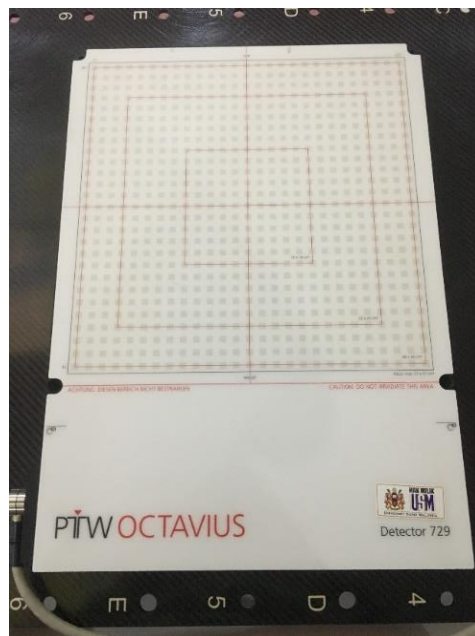


Figure 1.6: Example of ion chamber detector array system. A PTW 2D Array Seven29 ion chamber (PTW, Freiburg, Germany)

### 1.2.3 Method for patient specific IMRT QA for treatment verification

The gamma analysis method is used as a routine QA procedure for dose verification in IMRT treatment. The method provides good quantitative index of any discrepancy of dose delivered compared to the dose planned. The gamma index method was proposed by Low *et al.* provides a comparison between the calculated dose from the

planning and the measured dose which is obtained from the measurement of detector used [25]. The examined parameters in gamma index includes the distance to agreement (DTA) and dose difference (DD). The gamma is defined as the square root of a linear quadratic addition of the two examined parameters; DTA and DD in relative magnitude to their acceptance criteria  $C_{DTA}$  and  $C_{DD}$ , as shown in Eq.1

$$\gamma = \sqrt{\left(\frac{DTA}{C_{DTA}}\right)^2 + \left(\frac{DD}{C_{DD}}\right)^2} \quad (1)$$

The gamma index technique calculates the quantity of gamma,  $\gamma$ , for each point of interest using preselected DD and DTA. Then, the  $\gamma$  value is used to determine the pass-fail of the IMRT QA. For example, if the spatial difference in the DTA and DD results within the clinical acceptance criteria of 3 mm and 3% respectively then the gamma index is  $\leq 1$ , the criteria limits were not exceeded. However, if it  $> 1$ , the measurement result is outside the tolerance range. The percentage of points with  $\gamma$  value  $\leq 1$  is referred as gamma pass rate.

### 1.3 Geometrical uncertainties in radiotherapy

The highly conformal IMRT dose distributions are more sensitive to misalignments of the target with respect to the planned dose. The geometrical uncertainties are the most common factor which may affect the accuracy and precision of radiotherapy treatments especially for IMRT as it creates more complex treatment in order to deliver higher dose to the target volume and reduce toxicities to normal tissues [26,27]. The geometrical uncertainties can occur in term of patient setup and organ motions.

### 1.3.1 Margin recipe

The aim of radiotherapy treatments is to achieve high accuracy and precision of radiation delivery to the target. However, there are many sources of error that may occur during patient setup and treatment delivery that may affect the accuracy of radiotherapy treatment. Therefore, a margin is essential to make sure that the planned dose is delivered to the target.

There are various margin calculation methods proposed by researchers which are summarised in Table 1.1. The margin in this study is determined using Van Herk formula based on measured systematic error,  $\Sigma$ , and random error,  $\sigma$ , as shown in Table 1.1 [28]. The formula ensures 90% of studied patients receive a minimum cumulative CTV dose of at least 95% from the prescribed dose.

Table 1.1 Summary of published safety margin recipes for target (tumour) [29]

Author	Margin recipe	Assumptions
Stroom <i>et al.</i> 1999	$2 \Sigma + 0.7 \sigma$	95% dose to an average 99% of CTV tested in realistic plans
Van Herk <i>et al.</i> 2000	$2.5 \Sigma + 0.7 \sigma$	Minimum dose to CTV s 95% for 90% of patients
Mc Kenzie <i>et al.</i> 2000	$2.5 \Sigma + \beta(\sigma - \sigma_p)$	Extension of van Herk <i>et al.</i> for fringe dose due to limited number of beams

### 1.3.2 Image guided radiotherapy (IGRT)

Many technological inventions nowadays have resulted in significant progresses in radiotherapy planning, delivery, and verification including the integration of image guided modalities in the delivery of radiotherapy treatment. The IGRT can be defined as the use of frequent imaging in the treatment room immediately prior to beam delivery. The development of IGRT enables imaging of the tumour and patient setup immediately before IMRT treatment is delivered.

The systematic errors and random errors which might occur before and during treatment delivery can be reduced using IGRT. For example, if a patient is positioned incorrectly on the couch, a suitable correction was made to the couch position such that the patient can be treated according to the setup during treatment planning. However, if improper corrections were applied, there is a risk of missing the target volume. Missing the target during radiotherapy will result in tumour underdose which may potentially increase the dose to surrounding normal tissues.

IGRT uses CBCT to adjust target motion and positional uncertainties. A study has been done on the impact of IGRT on radiotherapy treatment workflow and the result showed that 95% out of 601 respondents of American Society of Radiation Oncology (ASTRO) reported the high prevalence of IGRT over other portal imaging [30].

IGRT also helps in reducing the PTV margin which allows possible dose escalation to tumour volume and enables surrounding healthy tissue to be spared [26,27,31]. From the study done by Chen *et al.* he proved that PTV margin can be safely reduced for HNC patients from 5 mm to 3 mm with no differences in locoregional control and distant metastasis-free survival using IGRT [32]. Den *et al.* has also proved that a 50% reduction in PTV margin for HNC patients could be achieved by demonstrating daily IGRT in IMRT treatments [33]. Thus, utilisation of IGRT during IMRT which is also known as IG-IMRT may help in reducing the risk of setup miss on HNC patients and treatment delivery of IMRT can further be improved with guidance from IGRT for a higher precision in beam delivery.

### **1.3.2 (a) Cone-beam computed tomography (CBCT)**

Cone beam CT (CBCT) is an effective IGRT tool for the verification of patient position. The tomographic slices from a patient are obtained through the kV



source/imager that are placed on the rotating linac gantry [34]. The volumetric data set in one gantry rotation is enabled with the usage of kV cone-beam.

The images from CBCT-based IGRT provide the setup errors of each patient and can be used to calculate the systematic and random error of the setup, and subsequently the PTV margin for patients with similar treatment setup. Example of gantry-mounted cone beam devices commercially available are the Elekta XVI (Elekta Medical Systems, Stockholm, Sweden) and Varian On Board Imager (OBI) (Varian Medical Systems, USA). X-ray source is one of the hardware components in CBCT. The x-ray source can either be in kV or MV. Each CBCT design has different target angle, travel range of the collimator and the focal spot values [35]. For example, the source of Elekta kV is a fan-cooled x-ray tube whereby the Varian OBI has an oil-cooled rotating anode x-ray tube. Other than x-ray source, flat-panel imager (FPI) is also a hardware component in CBCT. The FPI technology is based on the 2D matrix of amorphous silicon (a-Si) thin-film transistors (TFTs) on a scintillating material (Thallium doped Caesium Iodide) [36]. The scintillator is used for converting x-ray photons into light photons for the a-Si TFTs to convert to electrical signals and readout as digital signal. The projections of CBCT use the Feldkamp, Davis and Kress (FDK) algorithm. The measured cone-beam projections are pre-weighted, filtered and finally back projected along the same ray geometry used for forward projection [37].

### **1.3.2 (b) Correction strategies with image guided radiotherapy (IGRT)**

The correction strategies using IGRT are classified into online correction and offline correction. The online protocol compares the reference images from CT simulation with images from IGRT system taken in treatment delivery room. The protocol involves daily CBCT imaging and daily setup correction. The protocol measures the

difference as setup error and enables correction of the setup error for that treatment if it exceeds a designated threshold. This requires imaging, analysis and set-up correction before each fraction. A study done by Wang *et al.* showed that online correction can be effective at 2 mm threshold level [12].

On the other hand, offline protocol acquired images before treatment and matched to the reference image after the treatment is delivered. The CBCT image acquired on that day will be reviewed offline and the correction will be done for future fraction. This protocol aims to determine the individual systematic setup error, thus reduce it. Widely used offline correction protocols include No Action Level (NAL) and extended No Action Level (eNAL) protocols [38]. Even with the limited number of CBCT images, these correction protocols are able to reduce the systematic setup error which plays the biggest impact on the PTV margin.

Previous study related to offline IGRT protocol showed that the protocol helps in reducing systematic error. For example, de Boer *et al.* investigated the performance using Monte Carlo and compare the effect of eNAL in reducing systematic setup error between different natures of population; no transitions, large linear transitions and frequent large transitions [39]. From the study, they found out offline IGRT technique; eNAL protocol reduces the systematic error irrespective of time-dependent changes that may occur in population. Other study performed by Martens *et al.* also showed the ability of offline IGRT protocol in reducing systematic error. However, their study focused on rotational setup error instead of translation setup error [40].

## **1.4 Dosimetric impact of geometrical uncertainties on dose distributions**

Geometrical uncertainties in radiotherapy can cause a deviation between the calculated dose from TPS and the actual delivered dose distribution. As mentioned in section 1.3, the uncertainties mainly consist of patient setup error and internal organ motion.

The setup errors consist of systematic and random errors. Random errors may result in distorting the dose distribution. However, the impact on doses to the tumour and surrounding normal tissues is insignificant. This contradicts to the impact of systematic errors which may under dose or overdose both the tumour and normal tissues.

Therefore, this study also aims to analyse the impact of 2D translational setup errors in right-left (RL) and superior-inferior (SI) directions, if not corrected towards dose distribution. The setup error in anterior-posterior (AP) direction was not included in the analysis as the verification of IMRT was performed on ionisation chamber array detector (PTW, Freiburg, Germany). The acceptance of the treatment planning was also performed based on 2D analysis using gamma index and Dose-Volume Histogram.

## **1.5 Purpose of study**

The main objective of the study is to investigate the accuracy of treatment using IG-IMRT on head and neck cancer patients. Three sub-objectives are as follows.

- To assess the dosimetric accuracy of IMRT treatment using ionisation chamber array detector (PTW, Freiburg, Germany)
- To study the impact of geometrical accuracy on the delivered clinical IMRT treatments using IGRT
- To study the effect of geometrical uncertainties on dose distributions

## **CHAPTER 2 MATERIALS AND METHODS**

### **2.1 Radiotherapy and dosimetry system**

This section describes the radiotherapy linac and treatment planning system (TPS) used to plan and deliver IMRT treatment in this study, followed by the dosimetry system used for the patient specific IMRT QA prior to treatment. This section also describes the characterisation of the dosimetry system used for the patient specific QA. The result of the dose measured from the dosimetry system will be compared with the dose calculated from the TPS. It is important to perform the characterisation to ensure that the detector is functioning well as this detector will be used for patient specific pre-treatment QA. The detector has to be able to measure the dose accurately since it affect the accuracy and precision of the dose measured for the IMRT patient.

#### **2.1.1 Radiotherapy linac and quality assurance**

Radiotherapy beam was delivered from Elekta linac (Elekta Medical System, Stockholm, Sweden). The linac delivered 6 MV photon beam and was equipped with 160 Agility MLCs (Elekta Medical System, Stockholm, Sweden). The MLCs are arranged into two MLC banks, with each bank consist of 80 MLCs. The right and left MLC bank are termed as Y1 and Y2 respectively.

The CBCT mounted to the Elekta linac is called X-ray Volume Imaging (XVI). The XVI acquires and reconstructs the 3D image data simultaneously. Figure 2.1 shows the user interface to compare the acquired CBCT images from the patient setup with the reference image from CT scan during treatment planning [26]. The x (RL direction), y (SI direction), and z (AP direction) axis displacements are then corrected by moving the couch on which the patient is immobilised.



Figure 2.1: X-ray volume imaging (XVI) software

QA of the linac is important to ensure the accuracy of the radiation delivered from the machine. QA programme implemented for the linac has been adapted from the American Association of Physicists in Medicine Task Group (AAPM TG) number 142 [41]. The QA procedures included daily, weekly, monthly, and yearly QA test. The QA programme for the linac aims to assure that the calibration and baseline values acquired at the time of acceptance and commissioning with the machine characteristics do not deviate significantly.

The accuracy of IMRT treatment would be mainly affected by the linac dose output constancy. The dose output of the linac was checked daily using a Quickcheck device (PTW, Freiburg, Germany) that is an ionisation chamber cross calibrated with farmer ionisation chamber used to calibrate the linac.

The mechanical QA tests such as gantry/collimator angle indicators and localising laser were also performed to guarantee the mechanical accuracy of IMRT treatment.

Other than dose output constancy and mechanical performance, the MLC performance also play an important role to ensure the accuracy of IMRT delivery. For MLC QA, the picket fence leaf pattern was used. For this QA procedure, the measurements were performed at fixed gantry angle and a slit of  $2\text{ cm} \times 20\text{ cm}$  dimensions stopping every 2 cm were used to produce seven pickets.

Next, the accuracy of IGRT registration is also important in this study. Thus, the QA test aspect for IGRT system was also performed. The QA test was carried out by checking the accuracy of kV and MV CBCT registration.

### **2.1.2 Treatment planning system (TPS)**

The TPS used throughout this study was Monaco treatment planning system (Elekta Medical System, Stockholm, Sweden). Monaco TPS uses Monte Carlo algorithm for dose calculation and optimisation of IMRT plans.

### **2.1.3 Radiation detector for IMRT verification**

Ionisation chamber is considered the gold standard because of their precision, availability, and relative ease of use [42]. Therefore, the radiation detector used in this study was a matrix of  $27 \times 27$  ionisation chambers known as the 2D array seven29 detector (PTW, Freiburg, Germany). The detector consists of 729 ionisation chambers vented in a polymethyl methacrylate (PMMA) slab. Each cubic chamber has a size of  $0.5 \times 0.5 \times 0.5\text{ cm}^3$ , with a center-to-center spacing between 2 adjacent chambers of 1 cm, yielding a maximum field of  $27\text{ cm} \times 27\text{ cm}$ . Throughout the study, the PTW 2D array seven29 ion chamber will be referred as ionisation chamber array detector.

The Octavius phantom (PTW, Freiburg, Germany) is used with the ionisation chamber array detector to allow data acquisition from IMRT treatment. The phantom cross section has an octagonal shape. The shape is designed to tolerate a complex

rotational IMRT plan verification. The phantom is made of polystyrene with a physical density of  $1.04 \text{ g/cm}^3$ . The phantom has a  $30.0 \times 30.0 \times 2.2 \text{ cm}^3$  central cavity for insertion of the ionisation chamber into the phantom.

The Octavius phantom with ionisation chamber array detector was scanned using CT scanner and the images were exported into TPS. The CT scan images of both phantom and detector shown in Figure 2.2 will then be used in TPS for characterisation experiment and patient specific pre-treatment QA verification purposes.

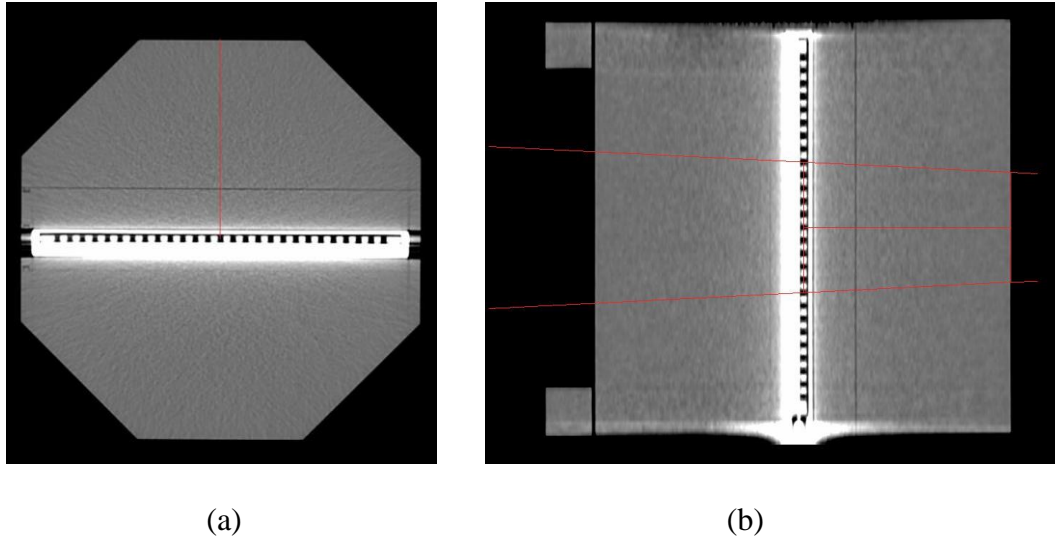


Figure 2.2: CT scan images of the phantom and detector from TPS (a) transverse plane (b) median plane

#### 2.1.4 Characterisation of the ionisation chamber array detector

There is a need to submit the ionisation chamber array detector to various tests in order to verify its level of reliability. Characterisation in term of dose rate dependency, linearity, reproducibility, SSD dependency, directional dependency and output factor will be studied comprehensively.



Before all the characterisation experiments were performed, the ionisation chamber array detector was inserted into the Octavius linac phantom as seen in Figure 2.3. The RS232 cable was connected to the PTW array interface before the PTW array interface was switched on. The cable transfers the measurements obtained on the 2D array to a computer with data acquisition software, Verisoft (PTW, Freiburg, Germany).

For characterisation of ionisation chamber array purpose, the measured dose from ionisation chamber array detector will be compared with dose calculated using TPS. Therefore, firstly, the scanned images shown in Figure 2.2 were imported into TPS. Then, the central ionisation chamber was contoured on the scanned image using TPS. All the treatment parameters that will be used for each characterisation experiments which will be described in Section 2.1.4(a)-(f) were planned on the TPS system and the resulted dose was calculated. The dose output calculated from the TPS was recorded and compared with the dose measured from the detector.

The phantom was setup perpendicularly to the in-room laser as shown in Figure 2.4. The gantry and collimator angles were also set to  $0^\circ$ . The SSD was kept at 84 cm. Then, the ionisation chamber array detector with Octavius phantom was calibrated using a cross-calibration procedure to calculate a cross calibration factor. A 200 MU was delivered on  $10 \times 10 \text{ cm}^2$  field size with a dose rate of 600 MU/min. This factor was then applied to the entire matrix.